

## INVESTIGATION OF LIQUEFIED NATURAL GAS (LNG) DISPERSION USING COMPUTATIONAL FLUID DYNAMICS

Izunna D. Udechukwu<sup>1\*</sup>, Siaka Dembele<sup>1</sup>, Ali Heidari<sup>1</sup>, Konstantin N. Volkov<sup>1</sup> and  
Jennifer X. Wen<sup>2</sup>

<sup>1</sup> School of Mechanical and Automotive Engineering, Kingston University,  
London, SW15 3DW, UK

<sup>2</sup> School of Engineering, University of Warwick, Coventry CV4 7AL, UK  
\*Corresponding author email: k1068315@kingston.ac.uk

**Key Words:** Computational Fluid Dynamics, Liquefied Natural Gas, Dispersion, Large Eddy Simulation, Reynolds-Averaged Navier–Stokes Equations.

**Abstract.** *Liquefied Natural Gas (LNG) is currently playing an important role in the global energy markets. This is evidenced by the growing demand and increased construction of LNG facilities across Europe and United States. One of the challenging problems within the LNG industry is to protect the general public from hazards which could result from accidental spill. A spill of LNG creates a flammable gas cloud which disperses through the atmosphere constituting fire and explosion hazards. The most commonly performed hazard analysis involves verifying compliance with regulations such as NFPA 95A. One method that is currently being used to establish compliance is dispersion modelling using Computational Fluid Dynamics (CFD). However, real terrain dispersion simulation presents unique difficulty due to issues related to complex turbulent phenomena development, particularly in the presence of obstacles such as buildings in the path of the dispersing cloud*

*The present study aims to demonstrate the potential of Large-Eddy Simulation (LES) for CFD simulation of LNG dispersion. For this purpose, ANSYS CFX is used to simulate LNG dispersion based on the Coyote Series Experiment. Turbulence in the flow field was prescribed via Smagorinsky sub-grid scale model originally developed for atmospheric turbulence. Under the Smagorinsky model, effect of adopting different closure models for Smagorinsky coefficient has been investigated. This include a constant value coefficient, the Wall damping closure (LES-WALE) and the scale-invariance closure (dynamic model).*

*Computational results are reported and compared with experimental data. Also, results were compared with those obtained from Reynolds-Averaged Navier-Stokes (RANS) simulations conducted as part of this study. Results of the simulations demonstrate that LES performs better than RANS in reproducing experimentally observed concentration trends. Of all three LES closure models of smagorinsky coefficient investigated in this study, the constant value approach with a Smagorinsky constant of 0.1 produced results which compare more favourably with experiment. The poor performance of the LES-WALE and LES dynamic models is thought to have resulted from the models being over-dissipative and under-dissipative respectively in the near-ground región.*

## 1 INTRODUCTION

A substantial amount of effort has been invested in the quantification of the level of hazard associated with accidental release of flammable gases. Earlier studies took the form of semi-empirical formulations generally referred to as integral or box models. Integral models which include SLAB and DEGADIS have been utilised in the studies of atmospheric gas dispersion. But these models have been widely criticised in the literatures on the grounds that assumptions limit their use to only prediction of dispersion over flat terrain. This means that integral models do not have the capability to account for the effect of obstacles such as buildings in the travelling path of the dispersing cloud.

Computational Fluid Dynamics is rapidly establishing itself as a reliable tool and possible replacement for integral models for dispersion modelling. CFD models account for the effect of obstacles on the path of the dispersing cloud making it suitable for simulations of practical dispersion scenarios [1,2]. Even though the use of CFD represents a substantial advancement, prediction of atmospheric dispersion of Natural Gas vapour continues to pose enormous challenge due to the complex physical processes involved. For instance, it is well known that a release of LNG will result in the formation of a flammable cloud whose dilution and transport relies heavily on ambient wind turbulence [3,4]. Considering that turbulence makes up a significant physics of the dispersion process, its accurate representation is critical in order to obtain reliable results. To account for turbulence effect, CFD tools incorporate a wide range of turbulent models with varying degrees of accuracy, computational cost and complexity. Also, each model more or less is specifically suited for different types of flow. For atmospheric dispersion, the wide range of scales associated with the atmospheric boundary layer makes it difficult to use the Direct Numerical Simulation (DNS) because it is highly computationally tasking to resolve these scales in real time. Reynolds Averaged Navier Stokes (RANS) models on the other hand is cheap computationally, but presents some challenging issues when used for LNG dispersion modelling. RANS resolves the mean flow and model the turbulence fluctuations by averaging over multiple snapshots or over long times thereby smooth out much of the eddies which results in substantial drop in computational effort required[5]. However, due to the averaging technique which underlies RANS models, they have been found to be ill-suited for capturing fluctuations in concentration over time. The UK Health and Safety Executive (HSE) relies on time varying concentration history to evaluate toxic load which they use for land use planning, hence Gant and Kelsey [6] specifically recommended using methods in which time varying concentrations are resolved.

Majority, if not all previous simulations of LNG dispersion have been conducted in the framework of RANS. Sklavounos et al[7], simulated Coyote Series experiment in CFX using RANS turbulence model. While it can be argued that the results obtained in their study were good in an average sense, predicted concentration time histories showed the inability of RANS to model concentration fluctuations. This resulted in intermittent wide gaps when compared qualitatively with the experiment. Later on, Hansen et al [8] simulated the Coyote experiment using FLACS, also in the framework of RANS. The results obtained were in acceptable agreement with experiments, although the wind inlet velocity was curiously changed from widely reported values for 'Coyote trial 5' which they simulated. Other

related works include those by Qi et al [9] in which the LNG spill test in the Brayton Fire Test Field (BFTF) were simulated with RANS turbulence closure. The results obtained were quantitatively in good agreement with experiment, but the quality of the results were adversely affected by RANS time averaging. Moreover, their results showed high sensitivity to source turbulence intensity whose value is usually specified arbitrarily in RANS to suit problem being solved. Gavelli et al [10] also encountered problems of source level turbulence intensity specification during a simulation of LNG dispersion. This prompted a subsequent work in which they proposed a formulation for the quantification of source turbulence intensity for use in RANS simulations[11]. However, the formulation was based on a single experiment and has not been benchmarked over a wide range of field experiments. More predictions of LNG dispersion in RANS framework are available in [3,12]

Somewhere between DNS and RANS lies an alternative turbulence model called Large-Eddy Simulation (LES). Instead of employing time averaging, LES utilizes a process generally referred to as ‘filtering’ to filter the equations of motion resolving eddies of length scale larger than the filter size and only model the eddies smaller than the filter size. Since only small scales are modelled, simulation results are less influenced by modelling errors. Also, time varying concentrations are captured since no time averaging is carried out with LES approach. However, LES models are more computationally demanding compared to RANS since time evolution of small scale motions are resolved in LES. Given the current development in computing power, the use of LES seems achievable in practice and has been explored in the present study. Thus, ANSYS CFX 14.0 has been used in this study to predict LNG dispersion based on the Coyote Series Experiment. A full description of the experiment can be found in [13].

## 2 LES FORMULATIONS

To separate the large scale motions from the small scale, LES applies a filtering operation producing a filtered variable denoted by an over bar as shown in equation 1. This process is better visualised as decomposition of the transport equations into two parts: the resolved part representing the large scale eddies which are solved for directly, and the sub-grid part represents the small scales whose effect on the resolved scales is included via a sub-grid scale model.

$$\bar{f}(x) = \int f(x') G(x, x'; \bar{\Delta}) dx' \quad (1)$$

Where  $G$  denotes the filter function and  $\bar{\Delta}$  denotes the filter width. Thus, all eddies of length scale less than the filter width are filtered out for modelling while eddies of other sizes are retained and resolved directly. However, most commercial CFD codes simplify LES calculations by using the grid size as the filter rather than perform explicit filtering, an approach generally referred to as box filtering.

### 2.1 The filtered governing equations

The equations that govern LNG dispersion consists mainly of the Navier-stokes equations, species transport equations and the energy equation. By applying the filtering operation to the governing equations, the filtered transport equations are obtained. For low mach number flows

such as LNG vapour dispersion, the incompressible form of the filtered equations can be used, but in a form that accounts for density variation [14] :

Continuity

$$\frac{\partial \bar{\rho}}{\partial t} + \frac{\partial(\bar{\rho} \bar{u}_i)}{\partial x_i} = 0 \quad (2)$$

Momentum

$$\frac{\partial(\bar{\rho} \bar{u}_i)}{\partial t} + \frac{\partial(\bar{\rho} \bar{u}_i \bar{u}_j)}{\partial x_j} = -\frac{\partial \bar{P}}{\partial x_i} + \frac{\partial(\bar{\tau}_{ij} + \tau_{ij})}{\partial x_i} + \rho g_i \quad (3)$$

Scalar transport

$$\frac{\partial(\bar{\rho} \bar{Y}_s)}{\partial t} + \frac{\partial(\bar{\rho} \bar{u}_i \bar{Y}_s)}{\partial x_j} = \frac{\partial}{\partial x_i} \left( \frac{\mu}{S_c} \frac{\partial \bar{Y}_s}{\partial x_i} \right) + \frac{\partial q_s}{\partial x_i} \quad (4)$$

Energy

$$\frac{\partial(\bar{\rho} c_p \bar{T})}{\partial t} + \frac{\partial(\bar{u}_i c_p \bar{T})}{\partial x_i} = \frac{\partial}{\partial x_i} \left( K \frac{\partial \bar{T}}{\partial x_i} \right) + \frac{\partial q_s}{\partial x_i} \quad (5)$$

Where  $\tau_{ij}$ ,  $\gamma_s$  and  $q_s$  denote sub-grid scale (SGS) stresses, sub-grid scale species fluxes and sub-grid scale heat fluxes respectively. The tilde denote Favre filtering which entails that density is variable for each time step. To close the set of equations, a closure model is usually adopted for the sub-grid terms. A number of modelling approaches exist in the literatures with the most widely used being the eddy-viscosity model in which the SGS terms are prescribed via a simplified Boussinesq approximation:

$$\tau_{ij} - \frac{1}{3} \tau_{kk} = -2\mu_T \bar{S}_{ij}; \quad \gamma_s = \frac{\mu_T}{S_{cT}} \frac{\partial \bar{Y}_s}{\partial x_j}; \quad q_s = \frac{\mu_T c_p}{p_{rT}} \frac{\partial \bar{T}}{\partial x_j} \quad (6)$$

Where  $\bar{S}_{ij} = \frac{1}{2} \left( \frac{\partial \bar{u}_i}{\partial x_j} + \frac{\partial \bar{u}_j}{\partial x_i} \right)$  denote the rate of strain tensor,  $S_{cT}$  is the turbulent Schmidt number,  $p_{rT}$  is the turbulent prandtl number and  $\mu_T$  is the sub-grid eddy viscosity. For solution purposes,  $\tau_{kk}$  is absorbed into the pressure term [15]. The values of the model parameters ( $S_{cT}$  and  $p_{rT}$ ) is well established in the literatures for isotropic turbulence [16]. The sub-grid eddy viscosity can be parameterised via the filtered strain rate  $\bar{S} = (2\bar{S}_{ij}\bar{S}_{ij})^{1/2}$  giving the well-known Smagorinsky model as shown in equation 7 below.

$$\mu_T = l_s^2 \bar{S} = (C_s \Delta)^2 \bar{S} \quad (7)$$

Where  $l_s$  is a characteristic scale which relates to the grid spacing ( $\Delta$ ) through the Smagorinsky coefficient  $C_s$ . There are currently three major versions of Smagorinsky models which differs from one another based on the formulation of the Smagorinsky coefficient. This include: (a) specifying the Smagorinsky coefficient as a constant value throughout the domain otherwise referred to as 'LES-Standard in this present study, (b) a traditional Smagorinsky coefficient closure that requires the specification of a wall damping function generally referred to as the LES-WALE, and (c) a stand closure that assumes scale-invariance (LES-Dynamic)

model. Full description of the three models is available elsewhere in [16,17] and will not be discussed in this study. All three models are available in ANSYS CFX 14.0 and have been assessed based on Coyote experiment in this present study.

**Table 1:** Summary of experimental conditions of Coyote Trials

Trial number	Wind speed (ms <sup>-1</sup> )	Temperature (°C)	Spilled volume (m <sup>3</sup> )	Spill rate (m <sup>3</sup> min <sup>-1</sup> )	Spill duration (s)
3	6.0	38.3	14.6	13.5	65
5	9.7	28.3	28.0	17.1	98
6	4.6	24.1	22.8	16.6	82
7	6.0	25.3	26.0	14.0	111

### 3 DESCRIPTION OF COYOTE EXPERIMENT AND CFD SIMULATION

The Coyote series of LNG spill experiment were conducted by Lawrence Livermore National Laboratory (LLNL) and Naval Weapon Centre (NWC) at China Lake, California, in 1981. The aim was to quantify LNG vapour cloud dispersion, and hence investigate the extent of vapour cloud fire that could result from different spill scenario. During these experiments, large quantities of LNG were spilled on water surface and the subsequent vapour dispersion monitored using multiple sensors placed at several locations downwind of the spill. The LNG was spilled in a 29m radius water test basin on to a splash plate placed at shallow depth in order to limit LNG penetration into water. Water level was 1.5m below the surrounding ground level. A total of ten experiments were performed majority of which involved the release of LNG, even though sufficient data for simulation set up is available only for three of the experiments (trials 3, 5 and 6). The release and weather conditions for each of the trials is as presented in table 1. For trial no 3 of the experiment, normal dispersion occurred for 100 seconds followed by rapid phase transition (RPT) phenomena.

#### 3.1. Simulation set-up in CFX

ANSYS CFX is a multi-purpose commercial CFD package capable of simulating a wide range of fluid flow problems through solving appropriate model equations using finite volume approach. For LES simulation of LNG dispersion, CFX solves the filtered governing equations (equations 2 to 5) to predict the time and space evolution of the dispersing cloud. However, before CFX can solve the set of governing equations, it requires a fully meshed geometry which is a prerequisite for every finite volume code.

Simulation set-up in ANSYS CFX therefore follows a basic procedure which consists of three major steps – creating the geometry and mesh, pre-processing (specification of boundary conditions etc) and solving (running the simulation).

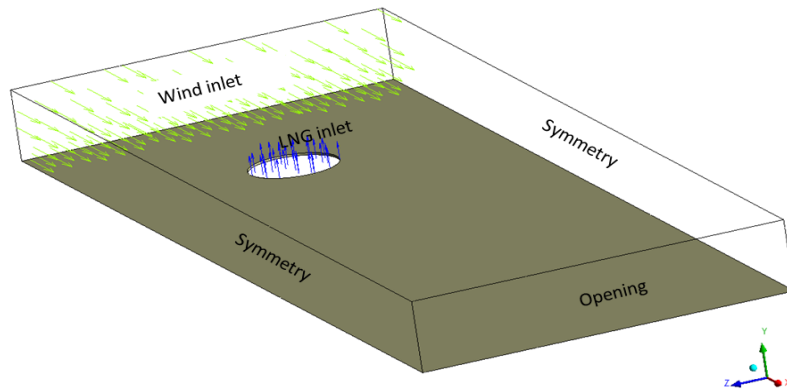


**Figure 1:** Computational domain and boundary condition

Construction of the computational domain was carried out in Gambit with dimensions 550 x 50 x 250 m in the windward, vertical and cross wind directions respectively. The domain was discretised using hexahedral cells for optimal computational efficiency. The mesh was selectively refined in the region of the spill and close to the ground as shown in figure 2, in order to improve accuracy in the region where mixing of air and LNG vapour initiates. The minimum horizontal cell size was 0.8m and minimum vertical cell size of 0.45m which guarantees aspect ratio is kept close to unity in the region of interest. In the horizontal plane, the grid expands away from the spill area but in a systematic manner in order to maintain aspect ratio within reasonable limit ( $0.2 \leq \text{aspect ratio} \leq 1$ ). The mesh for the entire domain consisted of 2142047 cells. Mesh sizes in the region of interest were chosen based on grid Independence guideline for LES simulations provided by Gant [18] in a previous study. Moreover, mesh sensitivity carried out showed that the abovementioned number of grids represents a good compromise between accuracy and computational cost.

At the wind boundary, velocity inlet boundary condition was specified with velocity set to represent the wind condition of the experiment as shown in table 1. Similarly, velocity inlet condition was specified at the LNG inlet boundary with an upward directed velocity of 0.0198 m/s. This velocity was calculated from the experimental spill rate, methane density and spill area. The temperature of the LNG was set equal to the boiling point of methane (111K) which is reasonable considering that methane is the major constituent of LNG. Also, methane is the most volatile constituent, hence vaporizing LNG is expected to consist mostly of gaseous methane thereby further justify the use of methane boiling point. Symmetry boundary condition was specified on the two side boundaries while opening type boundary condition was specified for both the outlet and top boundaries, with zero relative pressure and opening temperature set to atmospheric temperature recorded during the experiment. Opening type boundary condition allows fluid to flow both in and out of the domain, hence reducing the effect of insufficiently large domain on simulation results. Finally, the ground and the walls of the water test basin were specified as wall boundaries with a no-slip boundary condition which ensures zero gradient across the bottom of the domain.

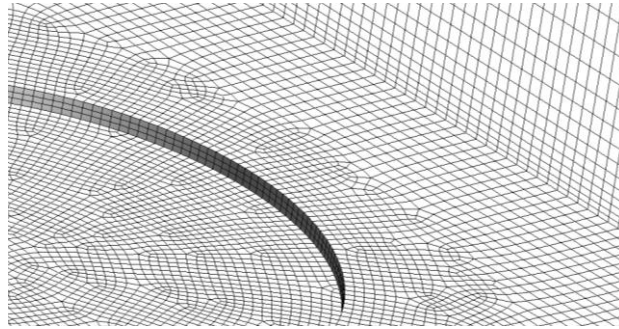


**Figure 2:** Computational grid

In addition to the boundary conditions specified, the transient calculation required that the domain be initialised. As a consequence, the simulation was carried in two stages. Firstly, a steady state simulation of wind flow to establish a fully developed atmospheric boundary layer. The essence of this approach was to obtain a site specific initial condition in which only wind flows initially before the injection of LNG. In the transient runs, the profiles of velocity and temperature obtained in the steady simulation was used to initialise the computational domain. The convergence criterion was the root mean square residual to be less than  $1e-4$  using a time-step size of 0.2 seconds. The complete execution for the transient dispersion simulation required about 20 hours real time on an Intel CPU with 2 processors running in parallel at 3.20Hz and 3.19Hz. The memory was 8GHZ RAM.

## 4 SIMULATION RESULTS

### 4.1 Baseline case-wind velocity profile development

The first part of the simulation comprises a steady state simulation to establish wind flow before the release of LNG. Figure 3 shows the vertical profiles of wind velocities at downwind locations 100m, 150m and 200m. As evidence from the plots, velocities in the near ground region where buoyant gas dispersion takes place does not change significantly, hence a fully developed wind profile was achieved prior to release of the gas. This entails that the gas was released into the correct wind environment

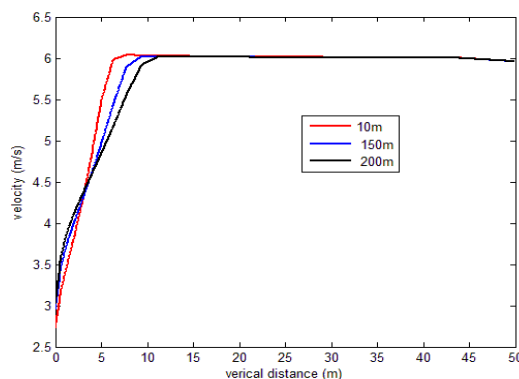


**Figure 3:** Predicted profiles of wind velocities at three downwind locations before the release of LNG.

## 4.2 Assessment of turbulent models

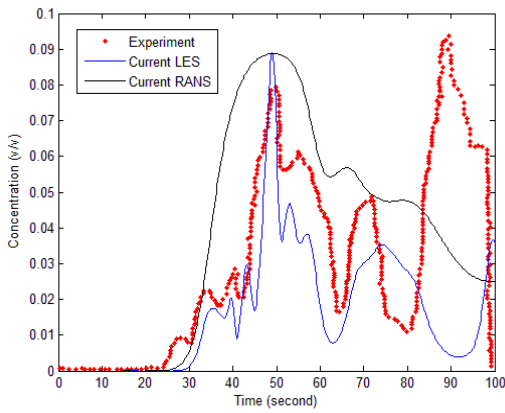
In Figure 4, representative of concentration time histories are shown based on results obtained from LES and RANS for coyote trial 3. The location of the gas detector (sensor) was 140m downwind from the spill center at a height of 1m above the ground level. It can be readily observed from the plots that both the RANS and LES simulations found good agreement with the experiment. The arrival time of the plume and the quantitative concentration histories was well captured by both turbulent models. But the LES model performed better in reproducing the trend observed during the experiment. For instance, the LES simulation performed well in capturing the fluctuations in concentration from the arrival time to time 100s, which represents the maximum time actual dispersion data was collected during the experiment without interference of rapid phase transition (RPT) which was observed afterwards. This ability to capture time varying concentrations is one of the typical strengths of LES over its time averaging counterpart

Figure 5 presents an assessment of the performance of the three existing closure models of Smagorinsky coefficient in predicting LNG dispersion. The models assessed include the standard model (LES-standard) which uses a constant value for the smagorinsky coefficient, the wall-adapted local eddy-viscosity model (LES-WALE) and the LES-Dynamic model. It is evident from the plots that the constant coefficient model produced result which is in better agreement with the experiment. The poor performance of the WALE model and the dynamic model may not be unconnected with the models being over-dissipative and under-dissipative respectively in the near ground region where LNG dispersion occurs.

## 4.3 Analysis of temperature and concentration evolution

Figures 6 and 7 represents volume rendered LNG volume fractions and contours of volume fractions respectively obtained in the present LES simulation. Interestingly, buoyancy effect has been well represented in the present simulation as evident in the results of volume fraction evolution. The plume emerges from the spill area, gain heat from the ambient wind which consequently reduces the density of the plume causing it to become positively buoyant as shown in figure 6. But as the parcels of gas move upwards into the high velocity region, at high enough wind velocity, their upward motion is counteracted producing an area of recirculation. This combined processes of dilution and strong wind counteraction dampens any upward motions causing the plume to revert to the near ground regions. The effect of the upward motion and dampening explains why contour plot of figure 7 shows a haphazard trend.

Figure 8 provides insight into the heat exchange and temperature variation that resulted to the buoyant behaviour exhibited by the dispersing cloud. As seen in the contour plots, the LNG plume emanated from underground with relatively low temperatures of about 134k which is typical of the release condition. As the plume evolves, turbulent mixing with ambient wind occurs causing the gas plume to gain heat from the ambient air and as a consequence experience temperature increase as it flows through the domain. This explains why temperatures are higher further from the spill area as shown in the temperature contour plots.



**Figure 4:** Experimental versus predicted LNG volume fractions for Coyote trial 3 at location 140m downwind of the spill center and 1m height.

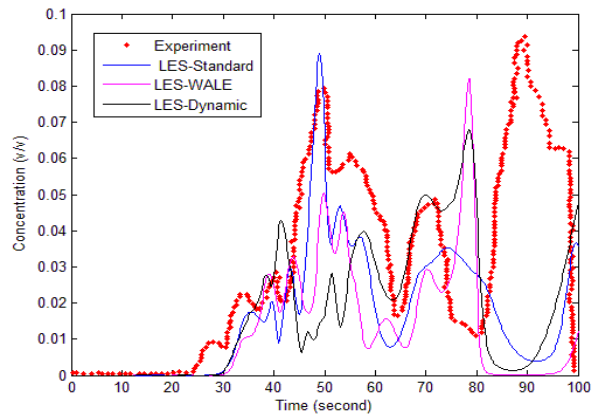


**Figure 5:** Assessment of three closure models of Smagorinsky coefficient (LES-standard i.e.  $C_s = 0.1$ , LES-WALE and dynamic models) through comparison with experimental measurements of LNG volume fractions for Coyote trial 3 at location 140m downwind of the spill center and 1m height.

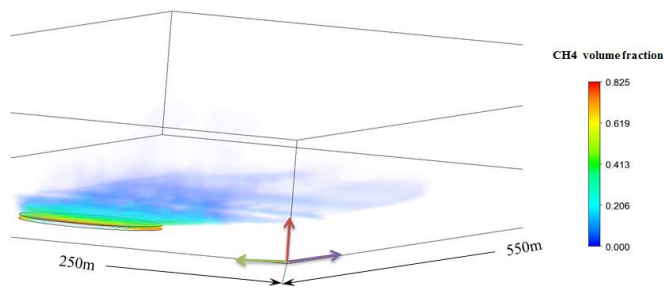


**Figure 6:** CFX volume rendered LNG volume fractions within the computational domain, for Coyote trial 3 prior to occurrence of rapid phase transition (100 seconds)

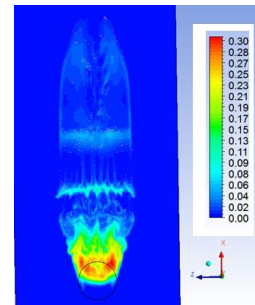


**Figure 7:** CFX predictions of LNG volume fraction contours at 1m elevation downwind, for Coyote trial 3 prior to rapid phase transition (100 seconds)

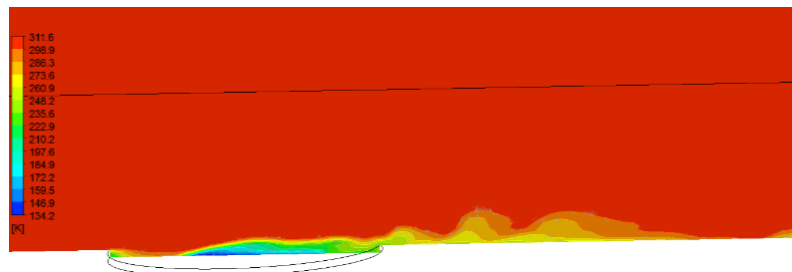


**Figure 8:** CFX predictions of temperatures in the vertical centerline plane downwind at time 100 seconds

## 5 CONCLUSIONS

A Computational Fluid Dynamics code (ANSYS CFX) has been applied to investigate vapour dispersion based on the Coyote LNG spill experiment. In general the predicted results show good agreement with experimental data leading to the conclusion that CFD can effectively describe the dispersion of flammable vapour following an accidental release of LNG. Also, the relative integrity of LES and RANS turbulence models in predicting LNG vapour dispersion was assessed by comparing experimental data with predicted results. While both models performed well in a quantitative sense, the ability of the LES model to capture time varying fluctuations has been identified to be a great asset as LES results showed better qualitative agreement with the experiment. This manifested in the classical way in which the trend in concentration time history were better reproduced using LES. The relative performance of three Smagorinsky LES models were also assessed. Results of the assessment put the standard model (constant coefficient) ahead of both the WALE and DYNAMIC models for LNG dispersion simulation.

## REFERENCES

- [1] B. R. Cormier, R. Qi, G. Yun, Y. Zhang, and M. Sam Mannan, "Application of computational fluid dynamics for LNG vapor dispersion modeling: A study of key parameters," *J. Loss Prev. Process Ind.*, vol. 22, no. 3, pp. 332–352, May 2009.
- [2] T. A. Melton and J. B. Cornwell, "LNG trench dispersion modeling using computational fluid dynamics," *J. Loss Prev. Process Ind.*, vol. 23, no. 6, pp. 762–767, Nov. 2010.
- [3] B. Sun, R. P. Utikar, V. K. Pareek, and K. Guo, "Computational fluid dynamics analysis of liquefied natural gas dispersion for risk assessment strategies," *J. Loss Prev. Process Ind.*, vol. 26, no. 1, pp. 117–128, Jan. 2013.
- [4] S. Sklavounos and F. Rigas, "Validation of turbulence models in heavy gas dispersion over obstacles," *J. Hazard. Mater.*, vol. 108, no. 1–2, pp. 9–20, Apr. 2004.
- [5] N. Jarrin, "Synthetic inflow boundary conditions for the numerical simulation of turbulence," A thesis submitted to the university of Manchester for the Degree of Doctor of Philosophy in the faculty of Engineering and Physical Sciences. 2008. .
- [6] S. E. Gant and A. Kelsey, "Accounting for the effect of concentration fluctuations on toxic load for gaseous releases of carbon dioxide," *J. Loss Prev. Process Ind.*, vol. 25, no. 1, pp. 52–59, Jan. 2012.
- [7] S. Sklavounos and F. Rigas, "Simulation of Coyote series trials—Part I:: CFD estimation of non-isothermal LNG releases and comparison with box-model predictions," *Chem. Eng. Sci.*, vol. 61, no. 5, pp. 1434–1443, Mar. 2006.

- [8] O. R. Hansen, F. Gavelli, M. Ichard, and S. G. Davis, "Validation of FLACS against experimental data sets from the model evaluation database for LNG vapor dispersion," *J. Loss Prev. Process Ind.*, vol. 23, no. 6, pp. 857–877, Nov. 2010.
- [9] R. Qi, D. Ng, B. R. Cormier, and M. S. Mannan, "Numerical simulations of LNG vapor dispersion in Brayton Fire Training Field tests with ANSYS CFX.," *J. Hazard. Mater.*, vol. 183, no. 1–3, pp. 51–61, Nov. 2010.
- [10] F. Gavelli, E. Bullister, and H. Kytomaa, "Application of CFD (Fluent) to LNG spills into geometrically complex environments," *J. Hazard. Mater.*, vol. 159, no. 1, pp. 158–168, Nov. 2008.
- [11] F. Gavelli, M. K. Chernovsky, E. Bullister, and H. K. Kytomaa, "Quantification of source-level turbulence during LNG spills onto a water pond," *J. Loss Prev. Process Ind.*, vol. 22, no. 6, pp. 809–819, Nov. 2009.
- [12] S. G. Giannissi, a. G. Venetsanos, N. Markatos, and J. G. Bartzis, "Numerical simulation of LNG dispersion under two-phase release conditions," *J. Loss Prev. Process Ind.*, vol. 26, no. 1, pp. 245–254, Jan. 2013.
- [13] R. D. Goldwire, H.C. Jr.; Rodean, H.C.; Cederwall, R.T.; Kansa, E.J.; Koopman, R.P.; McClure, J.W.; McRae, T.G.; Morris, L.K.; Kamppinen, L.; Kiefer, "Coyote series data report LLNL/NWC 1981 LNG spill tests dispersion, vapor burn, and rapid-phase-transition. Volume 1." 1983.
- [14] T. X. Qin, Y. C. Guo, and W. Y. Lin, "Large Eddy Simulation of Heavy Gas Dispersion around an Obstacle," in *Proceedings of the Fifth International Conference on Fluid Mechanics, Shanghai, China, 2007*, pp. 15–19.
- [15] N. Koutsourakis, I. C. Toliás, A. G. Venetsanos, and G. John, "Evaluation of an LES Code Against a Hydrogen," vol. 4, no. December 2012, pp. 225–236, 2013.
- [16] R. Stoll and F. Porté-Agel, "Dynamic subgrid-scale models for momentum and scalar fluxes in large-eddy simulations of neutrally stratified atmospheric boundary layers over heterogeneous terrain," *Water Resour. Res.*, vol. 42, no. 1, p. n/a–n/a, Jan. 2006.
- [17] F. Nicoud and D. F, "Subgrid-scale modelling based on the square of the velocity gradient tensor," *Flow, Turbul. Combust.*, vol. 62, pp. 182–200, 1999.
- [18] S. E. Gant, "Quality and reliability issues with Large-Eddy simulation," *HSE laboratory publications*. Accessed online on 3rd March, 2014 via:  
<http://s177835660.websitehome.co.uk/research/MSU200810.pdf>